Tension Force Estimation of Post-tensioning External Tendons Through Vibration-Based Monitoring: Experimental Validation

Javier Naranjo-Pérez[1,2(✉)] , Belén Vecino-Muñoz[1], Iván M. Díaz[1] ,
Carlos M. C. Renedo[1] , and Jaime H. García-Palacios[1]

[1] Universidad Politécnica de Madrid, Madrid, Spain
[2] Universidad de Sevilla, Seville, Spain
`jnaranjo3@us.es`

Abstract. There exists several methods to indirectly estimate pre-stressing forces in post-tensioning external tendons based on monitoring another relevant parameter. In this study, non-destructive vibration-based monitoring is employed to estimate their effective tension forces. A continuous monitoring of the tensioning process of a tendon installations on a 12-span concrete bridge for a high-speed railway is carried out using high sensitivity accelerometers distributed along the tendon. An operational modal analysis is then conducted for the signals at each stage of the tensioning process and the modal properties are extracted. Then, the effective tension force is estimated through a model updating of an analytical model of the tendon for each stage. The taut string model including bending effects is considered together with several boundary conditions: simply supported at both ends, clamped-simply supported and semi-rigid supports by including rotational stiffness of the connections. Thus, the tension force is estimated by minimizing a cost function defined in terms of the experimental and theoretical modal properties in terms of the natural frequencies and mode shapes. Finally, the estimated tension forces using different boundary conditions are compared with the measured ones given by the hydraulic unit during the tensioning process. A comparison between estimated and measured tendon forces including instantaneous losses along the tendon is carried out. That is, a discussion on friction losses (curvature friction and wobble coefficients) and the effect of the anchor set for the installed unbounded tendons is performed.

Keywords: Vibration-based monitoring · Operational modal analysis · Post-tensioning tendons · Tension force estimation · Prestress loss · Model updating

1 Introduction

External post-tensioning is commonly used in case of new bridge designs and in the framework of rehabilitations of in-service structures due to its ease of installation, re-stressing and substitution in case of failure. Hence, estimating the actual

tension force for safety and deterioration assessment with a reliable method is a current challenge. Among them, strain gauges, load cells or Fibre Bragg Grating sensors [1,5,8] can be found in the literature. Their main disadvantage is that they may not be applicable to existing structures, as they must be installed during construction. For those cases, direct measure of tension is not feasible and methods based on indirectly estimate it by means of another relevant parameter must be employed. The vibration-based methods have been extensively used due to their low economical cost, ease to use and accuracy [4,7]. These methods employ the relationship between tendon's tension and tendon's natural frequencies, which are obtained from the acceleration measurements [2,9]. However, in most cases the bending stiffness was neglected [12].

Several authors have proposed simplified formulas to identify the tension by using natural frequencies [10]. Herein, the taut-string theory including bending stiffness neglecting sag effects is used. The tendon model is defined considering three different models. Firstly, simply supported at both ends, so that there exists analytical expression for natural frequencies and mode shapes. The main drawback of this approach is that the approximation of the mode shapes near the supports is not accurate if the actual supports are different from the ideal pinned supports. To overcome this problem, an equivalent tendon with a shorter length (equivalent length) that fits better with the experimental mode shape is defined in order to deal with boundary uncertainties [3]. Second, semi-rigid supports by including rotational stiffness of the connections. In this case, the solution must be obtained numerically. Finally, clamped-simply supported which must be also solved numerically but presents less unknowns than the previous model.

The authors have carried out a continuous vibration-based monitoring of the tensioning process of a new tendon installation in a continuous concrete bridge of a high-speed railway line. For each tensioning stage, the tension force is inferred solving an optimization problem that minimizes the differences between numerical and experimental modal properties. Finally, the tension force applied at jacking (and considering losses) and the estimated one are compared. To compute the actual tension force at the segments, both friction losses and anchor set are considered in this sense, the performance of the method can be verified in a more reliable way.

2   Tension Force Estimation Method

Under this approach the tension force of the tendon is estimated from the measure of its natural frequencies and mode shapes (which are obtained from an operational modal analysis, OMA). The partial differential equation that governs the transversal displacement of a cable including bending stiffness is (i.e. tensioned Euler-Bernouilli beam) [11]:

$$EI\frac{\partial^4 v(x,t)}{\partial x^4} - T\frac{\partial^2 v(x,t)}{\partial x^2} + \rho\frac{\partial^2 v(x,t)}{\partial t^2} = 0 \tag{1}$$

where EI is the bending stiffness, $v(x,t)$ is the transversal displacement (tendon's deflection) at position x and instant time t, T is the tension force and

ρ is the linear mass density. Using the separation-of-variable method $v(x,t) = V(x)\cos(\omega t)$ and replacing it into the governing equation, the following ordinary differential equation is obtained:

$$EI\frac{\mathrm{d}^4V(x)}{\mathrm{d}x^4} - T\frac{\mathrm{d}^2V(x)}{\mathrm{d}x^2} - \rho V(x)\omega^2 = 0 \tag{2}$$

where ω is the angular frequency (rad/s). The solution of this equation is of the following form:

$$V(x) = C_1\cosh(r_1 x) + C_2\sinh(r_1 x) + C_3\cos(r_2 x) + C_4\sin(r_2 x) \tag{3}$$

where C_1-C_4 are integration constants and r_1 and r_2 are associated to the roots of the characteristic equation and have the following expressions:

$$r_1 = \sqrt{\frac{\sqrt{T^2 + 4EI\rho\omega^2} + T}{2EI}} \qquad r_2 = \sqrt{\frac{\sqrt{T^2 + 4EI\rho\omega^2} - T}{2EI}}. \tag{4}$$

2.1   Tendon with Pinned Joints

The first boundary condition considered in the analysis is the simply-supported which provides a closed-form solution of Eq. 3. However, real tendons may have certain rotational stiffness at their ends giving a poor approximation of the mode shape near the ends. For this reason, an equivalent pinned tendon with a reduced length (equivalent length) is considered [3]. That is, the mode shape of the actual tendon can be represented by the sinusoidal mode shape of the equivalent simply-supported tendon. Hence, the length of the equivalent tendon (L_{eq}), which is equal or lower than the actual one, remains as a key parameter to be determined.

In case of tendons hinged at both ends, Eq. 3 adopts the following form:

$$V(x) = \sin(r_2 x) \tag{5}$$

and finally, the i-th natural frequency and mode shape can be calculated according to:

$$f_i = \frac{i}{2L}\sqrt{\frac{T}{\rho} + \frac{\pi^2 EI i^2}{L_{eq}^2\rho}} \qquad i = 1, 2, \ldots, N \tag{6}$$

$$\phi_i(x) = \sin\left(\frac{i\pi x}{L_{eq}}\right) \tag{7}$$

N being the number of considered vibration modes. It is observed that the natural frequency depends on four parameters: the tension force, the bending stiffness, the linear mass density and the equivalent length.

2.2 Tendon with Semi-rigid Joints

Generally, the boundary conditions of tendon segments can be seen as semi-rigid connections in which a degree of rotational restraint takes place.

For the horizontal segments, the model of the tendon with rotational springs at the ends is used to verify the results of the equivalent length tendon model. In this case, Eq. 3 has to be solved numerically. For this purpose, the *fmincon* function from MATLAB software has been used to estimate the values for which the determinant of the boundary condition matrix is null (the so-called characteristic equation).

2.3 Tendon with Pinned and Clamped Joint

In cases where the equivalent length model leads to inaccurate results, the previous one with springs may be used. The main issue is that would involve more parameters to be estimated increasing significantly the computational cost. An alternative model is characterised by a clamped support at one end and a pinned support at the other end which may be coherent with the actual boundary conditions of inclined tendon segments (fixed at diaphragms and simply-supported at deviators). Under this assumption, the solution must also be solved numerically but the number of unknowns to be estimated is reduced.

2.4 Tension Force Estimation Approach

The methodology proposed in this study to estimate the tendon tension force uses a constrained multi-objective optimization problem that minimizes the discrepancies between the analytical modal properties and the experimental ones. The problem is stated as:

$$\text{find: } \boldsymbol{\theta} \qquad \text{to minimise } J(\boldsymbol{\theta}) = [J_1, J_2] \qquad \text{s.t.: } \boldsymbol{\theta}_l \leq \boldsymbol{\theta} \leq \boldsymbol{\theta}_u \qquad (8)$$

where $\boldsymbol{\theta}$ is the vector containing the parameter to be updated which depends on the considered model (always including the tension force), $\boldsymbol{\theta}_l$ and $\boldsymbol{\theta}_u$ are the lower and upper bounds of the parameters and J_1 and J_2 are two objective functions associated to the residuals between natural frequencies and mode shapes, respectively, and are defined as follows:

$$J_1 = \frac{1}{2}\sum_i^N \left(\frac{f_{i,num} - f_{i,exp}}{f_{i,exp}}\right)^2, \qquad J_2 = \frac{1}{2}\sum_i^N \frac{\left(1 - \sqrt{MAC}\right)^2}{MAC} \qquad (9)$$

where $f_{i,num}$ and $f_{i,exp}$ are the numerical and experimental natural frequencies, respectively, N is the number of vibration modes considered and MAC is the Modal Assurance Criterion which determines the similarity between mode shapes.

3   Experimental Campaign

The tensioning process was carried out in 4 stages (see Table 1), stressing at initial tendon's anchorage. Three of them were carried out in two steps due to technical reasons, resulting in 7 stages. Stage 0 consisted in an initial stressing at a 10% of the final tension force prior to grouting. The installed tendon is made up of 22 encapsulated strands with 7 wires each (inside an overall sheath filled with grout). At each stage the strands were stressed individually using a hydraulic mono-strand stressing jack. The tension force was gradually increased until the desired tension was reached and monitored from the hydraulic oil pressure.

Table 1. Stages of the tensioning process: duration and tension force (T_0) at the anchorage obtained by the hydraulic pressure.

Stage	Duration	T_0 (Anchorage) [kN]
0		450.00
1	2:07–2:31	1215.00
2.1	2:37–2:47	1546.22
2.2	2:50–3:19	2429.90
3.1	3:29–3:50	2982.20
3.2	3:53–4:18	3645.00
4.1	4:30–4:51	4028.70
4.2	4:55–5:22	4851.00

In order to identify the dynamic behaviour of the tendon and estimate the value of T (comprised of 9 segments in total over three spans), 22 high-sensitivity uniaxial accelerometers were placed at those nearer the anchorage to measure its vertical accelerations during the entire process. The instrumented segments of the tendon are shown in Fig. 1. Segment 1 was not measured due to security reasons, thus, Segments 2–5 made up the tested group. For the horizontal ones (Segments 2 and 5 of 22 m long), 9 equi-spaced accelerometers were used whilst the inclined ones (Segment 3 and 4 of 10.50 m long) were instrumented using 2 accelerometers, one at mid-span of the segment and the other at $L/8$ (L being the length of the segment) from mid-span.
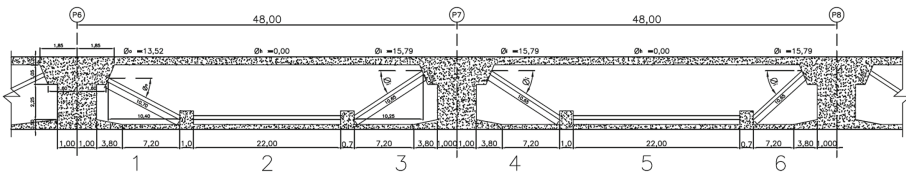

Fig. 1. General view of the tendon: instrumented segments.

For each stage, an OMA was conducted. The accelerometers were attached to the external polyethylene plastic pipe by ad-hoc braces (see Fig. 3a). The first four natural frequencies were tracked during the process. The software UPM-OMA created by the authors was employed for the analysis. First, signals detrending and filtering with a low-pass Butterworth filter with a cut-off frequency of 90 Hz was carried out. After that, they were decimated considering a decimation factor of 20 giving as result an effective sampling frequency of $5120/20 = 256$ Hz. The SSI-covariance-driven algorithm was used to conduct the OMA and extract the first four experimental natural frequencies and mode shapes of the tendon at each stage. Data during the tensioning process are not considered but only the temporal interval between the stages, f.i., the results of Stage 3.2 are computed using measurements from 4:18 to 4:30. Tables 2 and 3 show the first four natural frequencies of the horizontal and inclined instrumented segments, respectively. During the first stage, due to the low tension and installation reasons, the tendon was supported in its horizontal segments on sheaths as shown in Fig. 3b. That is why the OMA was not conducted for the Segment 5 for the mentioned stage. It is clear the increase of natural frequencies and the lower values of the segment closer the anchorage. Figure 2 shows the spectrogram of the first inclined instrumented segment (Segment 3) for the last four stages. It can be observed that the natural frequencies of the tendon increase with the tension force.
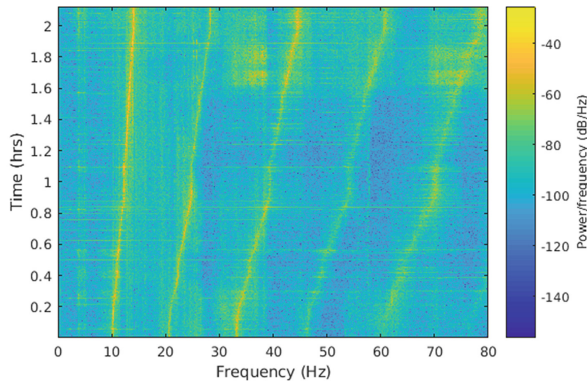

Fig. 2. Spectrogram of the Segment 3 for the last four stages of the tensioning process.

Once the natural frequencies and mode shapes are known, the tension force estimation process described in Sect. 2 is applied to each stage.

4   Tension Force Estimation and Discussion of Results

The methodology described in Sect. 2 is applied for the tension force estimation of the instrumented tendon for all the stages of the stressing process. The multi-objective minimization problem of Eq. (8) is solved using the genetic algorithm

Fig. 3. Measurements of the dynamic response of the tendon during the tensioning process: a) accelerometers attached to the tendon using ad-hoc braces and b) Segment 5 supported on sheaths during the first stage.

Table 2. Estimated experimental natural frequencies of the horizontal segments of the tendon at all the stages of the tensioning process.

Stage	Segment 2				Segment 5			
	f_1 [Hz]	f_2 [Hz]	f_3 [Hz]	f_4 [Hz]	f_1 [Hz]	f_2 [Hz]	f_3 [Hz]	f_4 [Hz]
1	3.89	7.09	10.97	14.96	-	-	-	-
2.1	4.10	7.96	12.16	16.52	4.09	8.32	12.68	17.01
2.2	5.14	10.15	15.38	20.88	4.80	9.66	14.66	19.89
3.1	5.55	11.06	16.63	22.62	5.18	10.43	15.94	21.50
3.2	6.26	12.37	18.66	25.24	5.93	11.75	17.83	23.35
4.1	6.57	13.14	19.77	26.74	6.21	12.54	18.86	25.40
4.2	7.14	14.22	21.38	28.80	6.73	13.52	20.41	27.46

Table 3. Estimated experimental natural frequencies of the inclined segments of the tendon at all the stages of the tensioning process.

Stage	Segment 3				Segment 4			
	f_1 [Hz]	f_2 [Hz]	f_3 [Hz]	f_4 [Hz]	f_1 [Hz]	f_2 [Hz]	f_3 [Hz]	f_4 [Hz]
1	7.18	15.13	25.02	35.84	7.10	15.05	24.39	35.15
2.1	8.00	16.56	27.12	38.32	7.93	16.53	26.50	37.70
2.2	10.20	20.73	33.20	46.24	10.18	21.03	32.80	45.88
3.1	10.99	22.28	35.60	49.16	11.04	22.60	34.94	48.96
3.2	12.31	24.82	39.42	54.08	12.36	25.25	38.79	53.68
4.1	13.05	26.30	41.55	56.88	13.12	26.70	40.73	56.39
4.2	14.12	28.30	44.73	60.76	14.15	28.72	43.93	60.16

programmed in the software MATLAB. The search range of the parameters were limited to reduce the computational cost. The linear mass density is derived from the geometry of the tendon and the material properties provided by the manufacturer, yielding $\rho = 45 \, \text{kg/m}$.

4.1 Friction Losses and Anchor Set

The tension force given by the hydraulic system at the anchorage is modified in accordance with the losses due to the friction. These are calculated as:

$$\Delta T(x) = T_0 \cdot \left(1 - e^{-(\mu\theta + \kappa x)}\right) \tag{10}$$

$\Delta T(x)$ being the loss due to friction at the point x under consideration, T_0 the tension force at jacking and μ and κ the friction coefficient and Wobble friction coefficient, respectively. These last coefficients are defined according to [6], taking the followings values: $\mu = 0.12$ and $\kappa = 0$ which correspond with unbounded tendons (the strands have are encapsulated individually). Considering these coefficients and the geometric parameters shown in Fig. 1, the friction losses are calculated using Eq. 10 and the tension force is derived. Table 4 shows the tension force at midspan of each segment obtained from the tension at jacking.

Table 4. Friction losses and tension force at each segment and stage of the stressing process.

Stage	T_0 [kN]	ΔT_2 [kN]	T_2 [kN]	ΔT_3 [kN]	T_3 [kN]	ΔT_4 [kN]	T_4 [kN]	ΔT_5 [kN]	T_5 [kN]
1	1215.00	38.75	1110.97	37.44	1073.53	72.51	1001.02	33.69	967.33
2.1	1546.22	49.31	1413.83	47.65	1366.18	92.28	1273.90	42.88	1231.03
2.2	2429.90	77.49	2221.85	74.88	2146.97	145.02	2001.95	67.38	1934.57
3.1	2982.20	95.11	2726.87	91.90	2634.96	177.98	2456.98	82.69	2374.29
3.2	3645.00	116.25	3332.92	112.33	3220.59	217.54	3003.05	101.07	2901.98
4.1	4028.70	128.48	3683.77	124.15	3559.61	240.44	3319.17	111.71	3207.46
4.2	4851.00	154.71	4435.66	149.49	4286.17	289.52	3996.65	134.51	3862.14

The selection of the optimum solution from the corresponding Pareto front leads to the values of the estimated tension force, which are collected in Table 5. For the horizontal segments, the simplified model considering the equivalent length was considered as a difference equal to 4% was achieved when compared to the model with rotational springs. The fixed-simply supported tendon model was employed for the inclined segments. This table also shows the relative error between the estimated experimental tension force and the calculated value taking into account the losses. These errors, which exceptionally could be high, are very small at the three last stages when tendon's tension reaches acceptable values and the tendon has the proper behaviour.

Table 5. Estimated tension force T [kN] and relative error [%] with respect to the experimental ones considering friction losses.

Stage	Segment 2		Segment 3		Segment 4		Segment 5	
	Estimated	Error	Estimated	Error	Estimated	Error	Estimated	Error
1	1078.64	−2.91	988.38	−7.93	838.87	−16.20	-	-
2.1	1444.23	2.15	1206.98	−11.65	1065.20	−16.38	1401.69	13.86
2.2	2328.40	4.80	2036.83	−5.13	2038.13	1.81	2073.36	7.17
3.1	2645.85	−2.97	2188.82	−16.93	2202.46	−10.36	2414.83	1.71
3.2	3522.79	5.70	2809.42	−12.77	2945.66	−1.91	3073.39	5.91
4.1	3819.34	3.68	3162.22	−11.16	3230.29	−2.68	3319.05	3.48
4.2	4504.34	1.55	3806.35	−11.19	3935.22	−1.54	3942.94	2.09

Analysis of the anchor set losses reveals that there is not any influence on the instrumented segments as the distance is lower than the length of Segment 1. For this segment, the value of the tension including friction losses would be reduced up to 6%. However, this fact could not be experimentally verified.

5   Conclusions

In this study, vibration-based monitoring has been applied to estimate the tension force of a post-tensioned external tendon. The method has been validated during the whole process of the tensioning of a new tendon on a railway bridge. More concretely, from the modal properties obtained through the OMA of the recorded accelerations, the tension force for each stage has been inferred by minimizing the differences between the experimental and the numerical modal properties. The first 4 vibration modes have been used in the tension estimation. The results were compared with the experimental ones provided by the hydraulic system and taking into account a model for the friction losses. The differences between the measured and estimated tension force were within the permissible tolerance taking into account the accuracy of the anchorage tension measure and the uncertainties on the friction losses model.

The proposed and validated methodology does not require drilling the sheath and the fact of considering the bending stiffness and more than one vibration mode leads to an accurate estimation of the tension force. For these reasons, it can be reliably used as an NDT method to estimate the in-service tension force of tendons. The fact of considering the bending stiffness and more than one vibration mode leads to an accurate estimation of the tension force. Furthermore, it can be simply and directly integrated into a SHM system that would allow instantaneous tendon tension monitoring.

References

1. Abdel-Jaber, H., Glisic, B.: Monitoring of prestressing forces in prestressed concrete structures—an overview. Struct. Control. Health Monit. **26**(8), e2374 (2019)
2. Casas, J.R.: A combined method for measuring cable forces: the cable-stayed Alamillo Bridge, Spain. Struct. Eng. Int. **4**(4), 235–240 (1994)
3. Chen, C.C., Wu, W.H., Chen, S.Y., Lai, G.: A novel tension estimation approach for elastic cables by elimination of complex boundary condition effects employing mode shape functions. Eng. Struct. **166**, 152–166 (2018)
4. Chen, C.C., Wu, W.H., Huang, C.H., Lai, G.: Determination of stay cable force based on effective vibration length accurately estimated from multiple measurements. Smart Struct. Syst. Int. J. **11**(4), 411–433 (2013)
5. Chen, L., Zhang, Q., Wu, M.: Principle and method of measuring cable tension in a cable structures. Ind. Constr. **36**(S1), 368–371 (2006)
6. European Technical Assessment: Post-Tensioning Systems, ETA-07/0035 2013 (2013)
7. Furukawa, A., Hirose, K., Kobayashi, R.: Tension estimation method for cable with damper using natural frequencies. Front. Built Environ. **7**, 603857 (2021)
8. Jia, Z.G., Ren, L., Li, D.S., Li, H.N.: Cable stretching construction monitoring based on FBG sensor. In: Sensors and Smart Structures Technologies for Civil, Mechanical, and Aerospace Systems 2011, vol. 7981, pp. 724–731. SPIE (2011)
9. Kim, B.H., Park, T.: Estimation of cable tension force using the frequency-based system identification method. J. Sound Vib. **304**(3–5), 660–676 (2007)
10. Le, X., Katsuchi, H., Yamada, H.: Asymptotic formulas for vibration-based cable tension identification accounting for uncertain boundary conditions. In: Bridge Maintenance, Safety, Management, Life-Cycle Sustainability and Innovations, pp. 3008–3015. CRC Press (2021)
11. Morse, P.M., Ingard, K.U.: Theoretical Acoustics. Princeton University Press, Princeton (1986)
12. Zhang, M., He, H., Li, G., Wang, H.: Fully automated and robust cable tension estimation of wireless sensor networks system. Sensors **21**(21), 7229 (2021)